International Journal of the Physical Sciences Vol. 6(15), pp. 3733-3744, 4 August, 2011
Available online at http://www.academicjournals.org/IJPS
DOI: 10.5897/IJPS10.250
ISSN 1992 - 1950 ©2011 Academic Journals

Full Length Research Paper

Spatial distributions and energy landscape of MinE protein dynamics via the biophysical spot tracking technique

Sitta Aroonnual[1], Waipot Ngamsaad[1,7], Paisan Kanthang[1,2], Narin Nuttawut[1,6], Wannapong Triampo[1,4,6]*, Darapond Triampo[3,6] and Chartchai Krittanai[5]

[1]R&D Group of Biological and Environmental Physics, Department of Physics, Faculty of Science, Mahidol University, Bangkok 10400, Thailand.
[2]Rajamangala University of Technology, Phra Nakhon, Bangkok 10800, Thailand.
[3]Department of Chemistry, Center of Excellence for Innovation in Chemistry, Faculty of Science, Mahidol University, Bangkok 10400, Thailand.
[4]Institute for Innovative Learning, Mahidol University, 999, Phuttamonthon 4 Road, Salaya, Nakorn Pathom 73170, Thailand.
[5]Institute of Molecular Biosciences, Mahidol University, Salaya Campus, Nakhon Pathom, Thailand.
[6]ThEP Center, CHE, 328 Si Ayutthaya Road, Bangkok, 10400 Thailand.
[7]School of Science, University of Phayao, Phayao 56000, Thailand.

Accepted 2 June, 2011

The MinCDE protein system is known to dictate cytokinesis cell division in prokaryotes by spatial regulation of the Z-ring. The oscillatory dynamics of MinC and MinD depends on the presence of MinE, where the MinE protein dynamics acts as a topological specificity to the midcell. In this work, the *Spot Tracking Technique* is used to determine the biophysical quantities of MinE protein dynamics, namely, diffusive motion, velocity distribution, spatial distribution, and energy profile. An alternative quantity that indicates the potential of the mean force characteristic function is proposed to be an effective potential parameter to indicate the optimal energy to generate a stable spatial-temporal pattern formation of MinE proteins. The localization and distribution patterns along the cell length were well confirmed, while other quantitative information related to MinE cluster positions have been revealed. In addition, the effective potential was found to relate to the spring-like potential. The minimum region indicates the potential cluster depth that occurs near the midcell zone, which corresponds to the finding that the MinE cluster is mostly concentrated at midcell.

Key words: Spot tracking technique, cell division, MinE proteins, protein oscillation.

INTRODUCTION

Cytokinesis in prokaryotes needs to be spatially regulated in order to ensure that it occurs between daughter genomes. In *Escherichia coli* (*E. coli*) and other rod-shaped bacteria, cytokkinesis is initiated by the tubulin-like GTP FtsZ in a polymeric ring at center of the cell that is called Z-ring (Lutkenhaus and Addinall, 1997; Rothfield et al., 1999). The midcell positioning of Z-ring is controlled by two major negative regulatory systems. The first system is called nucleoid occlusion, blocks Z-ring assembly in the cellular space that is occupied by nucleoid mass (Woldringh et al., 1991; Yu and Margolin, 1999). The other system consists of three proteins, MinC, MinD, and MinE, which prevent Z-ring assembly at the cell poles (de Boer et al., 1989; Rothfield et al., 2001).

*Corresponding author. E-mail: scwtr@mahidol.ac.th, wtriampo@gmail.com. Tel: 662 441-9816 ext. 1131. Fax: 662 441-9322.

MinC colocalize and cooscillate with MinD (Hu and Lutkenhaus, 1999; Raskin and de Boer, 1999b) which acts together as a negative regulator of Z-ring assembly, and oscillatory dynamics depends on MinE (Hu and Lutkenhaus, 1999; Raskin and de Boer, 1999a, 1999b). MinCD complex prevent the correct interaction of FtsA with the FtsZ ring *in vivo* (Justice et al., 2000), and MinC has been shown to inhibit FtsZ polymerization *in vitro* (Hu and Lutkenhaus, 1999). Thus, the inhibition of polar division seems to be achieved by transiently disrupting assembly of the division machinery at each cell pole in an alternating manner. MinE provides topological specificity to the division inhibitor. In absence of MinE, MinC/MinD are distributed homogeneously over the entire membrane, resulting in a complete block of Z-ring formation and consequent formation of long filamentous cells that fail to divide into two daughter cells (Hu and Lutkenhaus, 1999; Raskin and de Boer, 1999a, 1999b; Rowland et al., 2000).

Although there are many experimental studies in the spatial-temporal pattern formations and the biochemical basis functions of Min system (Rothfield et al., 2005; Shih and Rothfield, 2006), only few reports provide the quantitative information especially MinE protein dynamics. Recently, Janthon and co-workers (Janthon et al., 2008) studied the quantitative information of MinE cluster dynamics by using the Single Particle Tracking technique (SPT). They demonstrated the pattern formation of MinE cluster and presented the spatial distribution of MinE proteins in terms of Gaussian distribution. For more quantitative information and biophysical quantities of this system, Unai et al. (2009) applied Spot Tracking Technique (STT) to MinD protein dynamics. They characterized the dynamic properties of MinD protein such as spatial distribution, velocity distribution and diffusive motion. They found that the MinD cluster performed subdiffusion for the half cell length with the dynamic exponent approximation in 0.34±0.18. These quantities for MinE dynamics are still unrevealed.

SPT or STT are based on the computer-enhanced video microscopy that have been developed to measure not only the movement of small molecules or particles, but also the trajectory of the molecule cluster and protein crowding (Saxton and Jacobson, 1997; Sage et al., 2005; Golding and Cox, 2006; Unai et al., 2009). These techniques have been used mostly in data analysis in order to classify the modes of motion (e.g. normal diffusion, anomalous diffusion, confined motion *etc.*) and to find the distribution of quantities character in the molecular motion.

In this work, we applied the STT to MinE protein dynamics in the subject of the shortcoming in biophysical quantities including diffusive motion, velocity distribution, spatial distribution, and energy profile. These quantities are very importance to understand the intracellular dynamics and functions importantly in terms of space and time scale interaction. We used the diffusive motions and velocity distributions to characterize the correlation motion of MinE that implies the time scale interaction of MinE dynamics. We also used the spatial distribution and energy profile to characterize the local properties of MinE proteins. These quantities are involved in the interaction region/zone of MinE protein dynamics in the cell and topological marker that acts as a midcell. We proposed the alternative quantity, called the energy profile. It indicates the potential of mean force characteristic function or interaction strength profile that respond to the MinE cluster motion. Moreover, the effective potential parameter may indicate the optimal energy to generate the stable spatial-temporal pattern formation of MinE proteins.

MATERIALS AND METHODS

Bacterial strain and growth conditions

E. coli strain RC1/pSY1083G [Δ*min*/P_{lac} - *ΔminC ΔminD ΔminE ::gfp*] was kindly provided by Yu-Ling Shih (Department of Microbiology, University of Connecticut Health Center) (Shih et al., 2003). For expression of MinE labeled with green fluorescent proteins (GFP), a starter of RC1/pSY1083G cells was grown in Lysogeny broth (LB) medium, 50 μg /ml ampilcillin, 25% glucose at 37°C and shaken overnight at 250 rpm. 1% of the overnight culture was then taken to grow in the new medium until the $OD_{600\ nm}$ was approximately 0.3 to 0.4. The centrifugation was performed at 3,000 rpm for 15 min to collect the cells. Cells were then re-suspended for at least 30 min in the same medium containing 0.1mM isopropyl-β-D-thiogalactopyranoside (IPTG) for protein induction. The cell culture was diluted with media before use. In our experimental preparation, 5 to 7 μl of sample was dropped onto a glass slide coated with 5 μl of poly-L-lysine (0.1%), then covered by a cover slip at room temperature (25°C) before examination.

Image acquisition and spot tracking technique

For fluorescence image sequences, a Zeiss Axioskop2 microscope and A-plan 100x/1.25 oil lenses were used with *in vivo* software support with exposure times of 900 ms. A charge-coupled device (CCD) camera (Evolution QEI monochrome) was attached to the video port of the microscope to acquire images and movies at 1 frame/s. After that the spot tracking technique (STT) was used to follow the region of interest (ROI) which gave off the highest GFP-MinE concentration signal. This highest signal is a representation of the cluster protein in the cell, which indicates the ring-like structure of MinE. The data obtained from the measurements were supported by the SpotTracker Java plug-in for the public domain ImageJ software. However, more details on image processing and tracking procedure are shown in Unai et al. (2009). SpotTracker is a robust and fast computational procedure to track fluorescent particles attached to the molecule of interest in time-lapse microscopy. This tracking provides the time series data as a text file (*x, y* coordinates) for the position of the ROI of the cluster protein, and detects ROI as a small neighborhood (3×3 pixels). More details of this tracking as a time algorithm can be found in Sage et al.

(2005). The acquired positions were analyzed by MATLAB software to calculate the physical quantities, including time memory, transport mode, spatial probability density, and energy profile.

Data analysis

GFP-MinE cluster motion and pattern formations

According to the position profile shown in Figure 2A(top), we calculated the velocity of GFP-MinE cluster as follows: $\vec{v}_i = \frac{\Delta \vec{r}_i}{\Delta t}$, where Δt = 1 s and i = number of frame, as shown in Figure 2A (bottom). For the period calculation of GFP-MinE oscillation, we focused on the absolute values of velocity of the GFP-MinE cluster. We looked for the time at the cluster when GFP-MinE switched from pole to midcell, collecting the information by using MATLAB script; then we plotted the switching time versus the index of switching time shown in Figure 2B. The slope from this graph relates to the average of the half oscillation period. In order to classify the motion of a particular GFP-MinE cluster from the midcell zone to the polar zones, a time series of its position $\vec{r}(t) = (x(t), y(t))$ was recorded in the new data sets by using the midcell position to separate the trajectory data into two data sets. According to these data sets, we calculated the mean squared displacements (MSD: $\left\langle \left|\Delta \vec{r}\right|^2 \right\rangle$). The average was taken over time within a single trajectory as follows (Qian et al., 1991; Saxton and Jacobson, 1997; Suzuki et al., 2005; Jin et al., 2007):

$$MSD(n\Delta t) = \frac{1}{N-1-n}\sum_{i=1}^{N-1-n}\left\{\left[x(i\Delta t + n\Delta t) - x(i\Delta t)\right]^2 + \left[y(i\Delta t + n\Delta t) - y(i\Delta t)\right]^2\right\}$$

where $x(t)$ and $y(t)$ are the GFP-MinE cluster position at time t ; N is the total number of frames; n is the number of the time interval which relates to time lag; and i is the positive integer.

According to this property, we distinguished the diffusing particle characteristics by using the relation between MSD and time lag. For linear profiles, the MSD of a diffusing particle varies with time as $\left\langle \left|\Delta \vec{r}(t)\right|^2 \right\rangle = 4D_\alpha t^\alpha$ (for 2D), where the dynamic exponent α distinguishes the type of diffusion encountered; $\alpha = 1$ indicates normal Brownian diffusion; $0 < \alpha < 1$ indicates subdiffusion; and $\alpha > 1$ indicates superdiffusion (Saxton and Jacobson, 1997; Metzler and Klafter, 2000; Tolic´-Nørrelykke et al., 2004; Golding and Cox, 2006). For parabola profiles, we considered the diffusing particle in terms of the fractional diffusion-advection second moment under Galilei invariance. This relation is followed by $\left\langle \left|\Delta \vec{r}(t)\right|^2 \right\rangle = 4D_\alpha t^\alpha + v^2 t^2$, where D_α is the effective diffusion coefficient and v is the velocity field (Metzler and Klafter, 2000; Kramers, 1940).

Energy landscape and localization analysis

The position series data were analyzed by a scattering plot of position (x,y) in terms of the normalization of length scale (diameter and cell length). We plotted the histogram of position along the normalized cell length; it indicated where the MinE cluster molecules were located. This result represented the probability density of the MinE cluster molecule ($P(x)$). In addition, we calculated the apparent effective potential from $U(x) = -k_B T \log(P(x))$, where $U(x)$ is the effective potential (Ritchie et al., 2005; Daumas et al., 2003; Jin et al., 2007; Haken, 1977) and $P(x)$ represents the probability density of MinE cluster molecules, which were calculated from the histogram with small bins (~3% or 0.03 of normalized cell length).

RESULTS

During image analysis, we found that the raw image sequences were very noisy or full of unwanted signals, as is evidently shown in Figures 1A and B. It was even clearer when we considered the surface plots (Figures 1A' and B'). This noise could reduce the efficiency of STT and needed to be reduced or eliminated. To do so, we used the Gaussian filter and image enhancement. Hence the noise signals were "cleaned" up as seen in Figures 1C, C', D and D'. The intensity signals became very sharp when compared with the raw image sequence (Figures 1A and B).

In addition, we analyzed the intensity signal of the sharp image sequence along the cell length, as shown in Figure 1E. We found that the intensity profiles clearly demonstrated the oscillation pattern of GFP-MinE. The peaks of the intensity profiles indicate the representative position of GFP-MinE cluster movement along the cell length. This tracked spot biologically represents the ring-like structure of MinE proteins. For quantitative characterization, we applied the STT to the image sequence based on tracking the center of the GFP-MinE cluster (3×3 pixels). This step provided us the data of MinE protein positions over time (Unai et al., 2009)). The position series at successive time points could then be used to determine several dynamic quantities, such as the trajectory as shown in Figure 1F.

Spatial-temporal pattern formation analysis

Using the intensity pattern formation in Figure 1E, we obtained the position profile as shown in Figure 2A (top). This elucidated the moving path and characteristic pattern of GFP-MinE cluster along the cell length. We found that GFP-MinE clusters typically move and spend time in the area from the midcell zone to the polar zone, swiftly switching from polar zone to midcell. We calculated the derivative of this moving path to get the velocity time evolution, as shown in Figure 2A (bottom). Consequently, the velocity profile led us to distinguish three velocity modes: (1) Switching velocity, the velocity of a GFP-MinE cluster that moves from the polar zone to

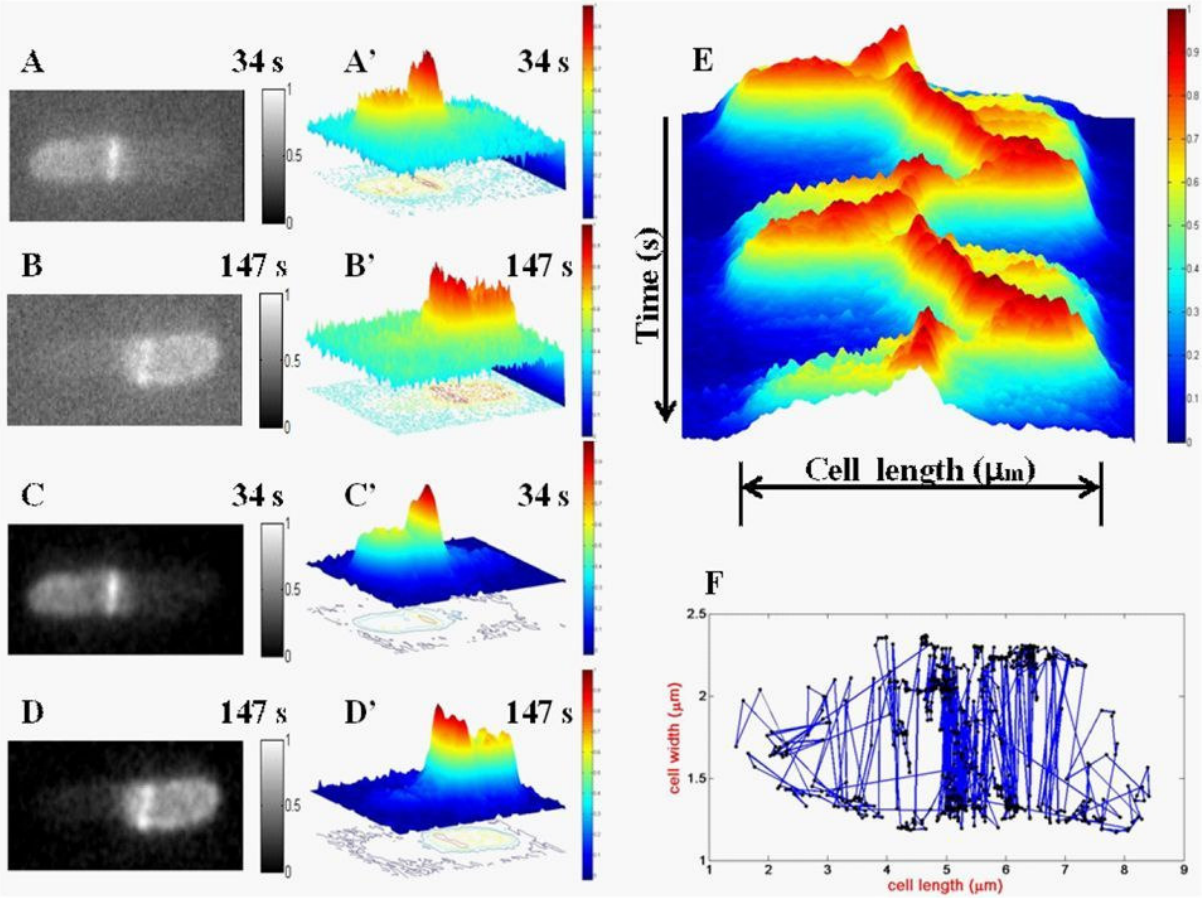

Figure 1. Image analysis and STT results for *E. coli* strain RC1/pSY1083G [Δ*min*/P$_{lac}$ - *ΔminC ΔminD ΔminE ::gfp*]]. (A and B) sample of a raw fluorescent image at 34 and 147 s, respectively. (A', B') The intensity plot of fluorescent images corresponding to A and B. The small peaks reflect the noise that is distributed over the image. (C and D) The fluorescent image in A and B after processing. (C', D') The intensity plot of fluorescent image corresponding to C and D. (E) The profile of the intensity pattern along cell length (0 to 600 s). This figure demonstrates the possible cluster position along cell length. (F) GFP-MinE cluster trajectory for the successive time of 800 s. For each intensity plot, the different colors of the contour plot represent the different intensity scale of GFP-MinE. All color scales in these figures perform in terms of normalization.

midcell zone (1.96±0.8 μm/s); (2) localized switching velocity, the velocity of a GFP-MinE cluster that moves during the switching period from the midcell to the edge or polar zone (0.46±0.15 μm/s), and localized velocity, the velocity of a GFP-MinE cluster that moves along the edge of cell in a path from the midcell to polar zone; 0.04±0.02 μm/s). From these behaviors, we determined two parameters to characterize the moving path, including ring structure moving time (RSMT) and ring structure moving length (RSML).

RSMT indicates the time interval for a GFP-MinE cluster moving from the midcell zone to the polar zone. This parameter leads to the measurement and approximation of the oscillation period of MinE proteins. In order to define the MinE oscillation period, we used both pattern formations of moving path and velocity time evolution.

The oscillation period of MinE is given by two RSMTs on a moving path related to 3 velocity peaks on the velocity time evolution. From this period definition, we measured RSMTs via the velocity peaks. The relation between RSMTs and switching events (or events of velocity peaks) is shown in Figure 2B; each RSMT performs the half oscillation period; the slope of red line in the figure indicates the average of half oscillation period. The RSMTs are approximately 133.25±62.7 s. For our experimental data, the oscillation period of GFP-MinEs is approximately 238±97 s (18 cell samples).

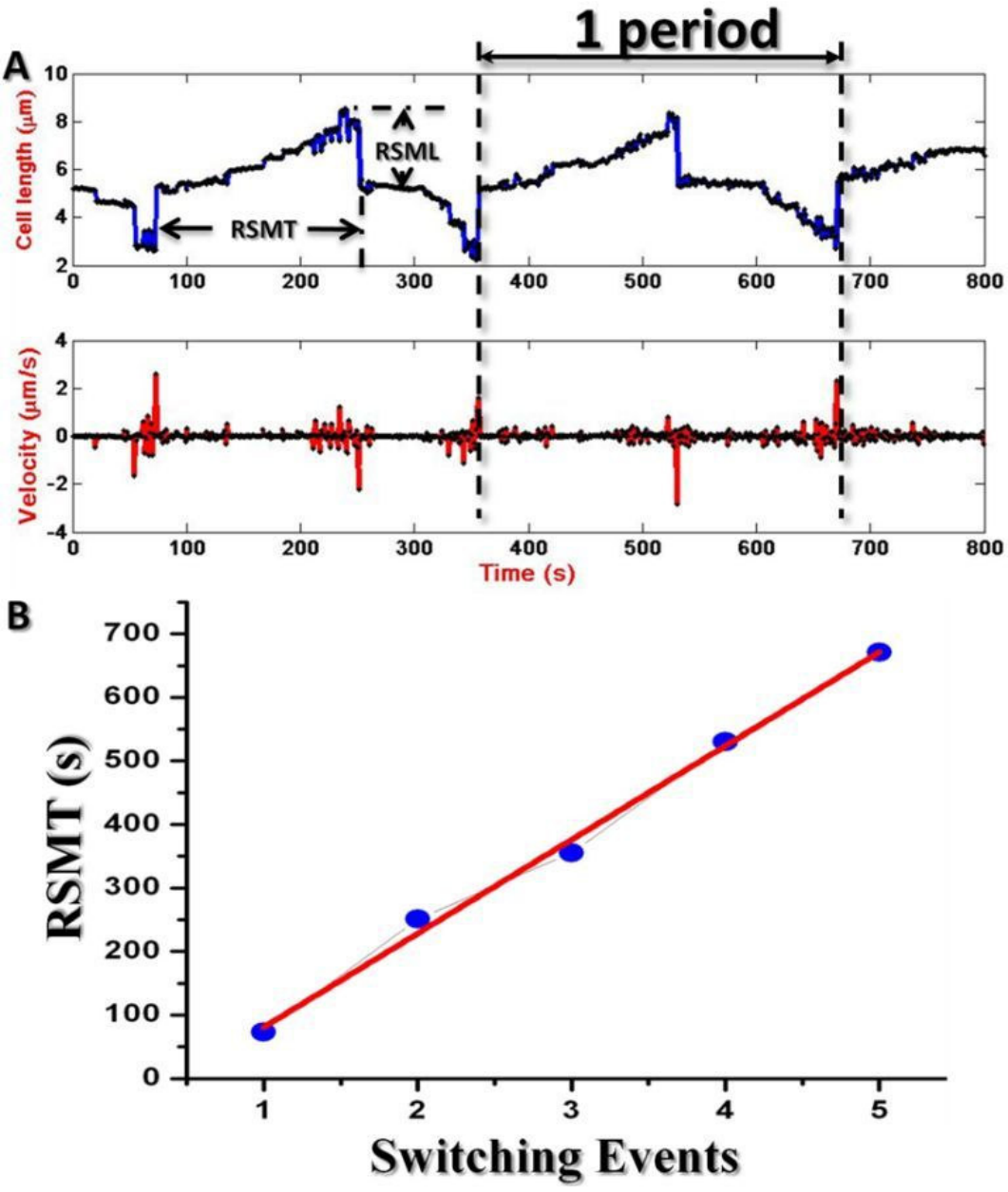

Figure 2. An example of the dynamics pattern and period of GFP-MinE along cell length (A) The oscillation pattern (top) and velocity time evolution (bottom) for an acquisition time of 800 s. RSMT corresponds to the half oscillation period. RSML performs the jump length from polar zone to midcell zone that corresponds to half of cell length. The oscillation period of GFP-MinE is defined by 2 RSMTs and 3 velocity peaks. (B) The relation between RSMT and switching events. Blue circles indicate the data points that correspond to each RSMT. Red line represents the fitting curve. The slope of this graph corresponds to the average period of half oscillation.

This result corresponds to previous reports (Fu et al., 2001; Hale et al., 2001) that directly measured the oscillation period via image sequence. However, our oscillation period was clearly measured by the oscillation pattern and its period definition, which led to increased precision of the dynamical time scale related to the biochemical kinetic interaction of Min proteins, especially from midcell to the polar zone.

RSML represents the moving length between the polar zones to midcell zone. This parameter indicates the

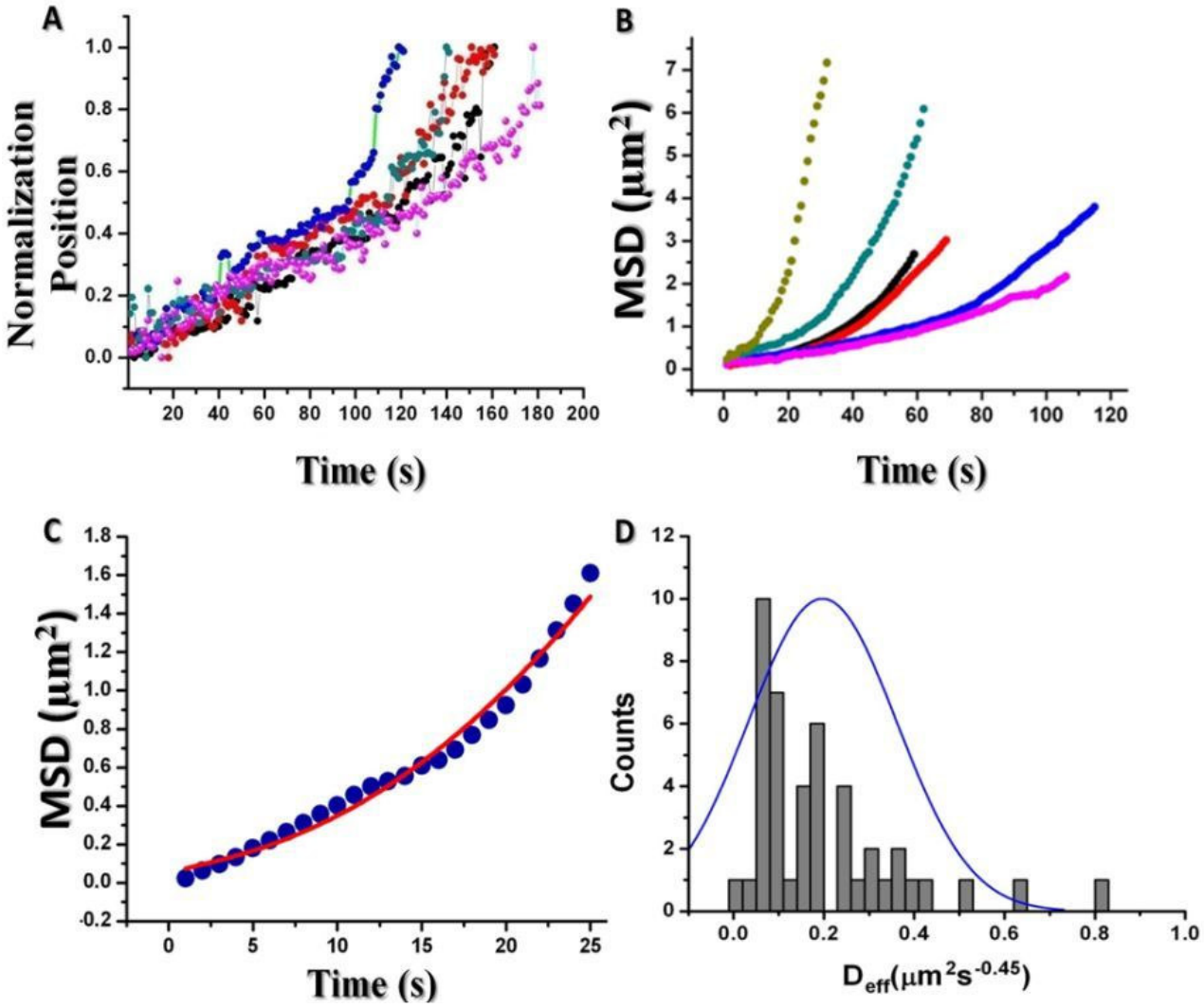

Figure 3. Position profile and MSD of GFP-MinE cluster. (A) Shows the normalized position profile for 5 sample paths. (B) Shows the MSD that corresponds to the data set in (A). (C) An example of MSD data (blue dots) and fitting curve (red line, R^2~0.98). The fitting function is the fractional diffusion-advection second moment (material and methods). The dynamic exponent for this curve is approximately 0.29. The other parameters are $4D_\alpha$ ~ 0.018 and v ~ 0.046. (D) The histogram for the effective diffusion coefficient with the average time scale 0.45. Blue line represents Gaussian function fitting. The average of the effective diffusion coefficients (D_α) is approximately 0.20±0.16 $\mu m^2/s^{0.44\pm0.25}$.

length scale that corresponds to the site specific function of MinE, which mostly moves to the midcell zone after the MinD-depolymerization process at the polar zone (King et al., 2000; Taghbalout et al., 2006). RSMLs are approximately 2.39±0.699 μm (for cell length approximately 5.1±0.8 μm).

From our analysis, as seen in Figure 3A (for 5 moving paths), we could distinguish GFP-MinE cluster motion between midcell and polar zone in terms of a normalization scale. MSD indicated that moving paths feature directed motion, as is evidently shown in Figure 3B. The curves could be fitted with the fractional diffusion-advection second moment (Metzler and Klafter, 2000); $\left\langle \left| \Delta \vec{r}(t) \right|^2 \right\rangle = 4D_\alpha t^\alpha + v^2 t^2$ with α = 0.44 ± 0.25 and R^2~0.92 (for 10 cell samples); An example is shown in Figure 3C. In addition, we evaluated the effective diffusion coefficient as shown in Figure 3D. This result cannot fit with the Gaussian distribution.

Next, we analyzed the velocity and velocity distribution throughout the cell, as shown in Figure 4A (for 10 cell samples). We fitted the data with two distribution functions.

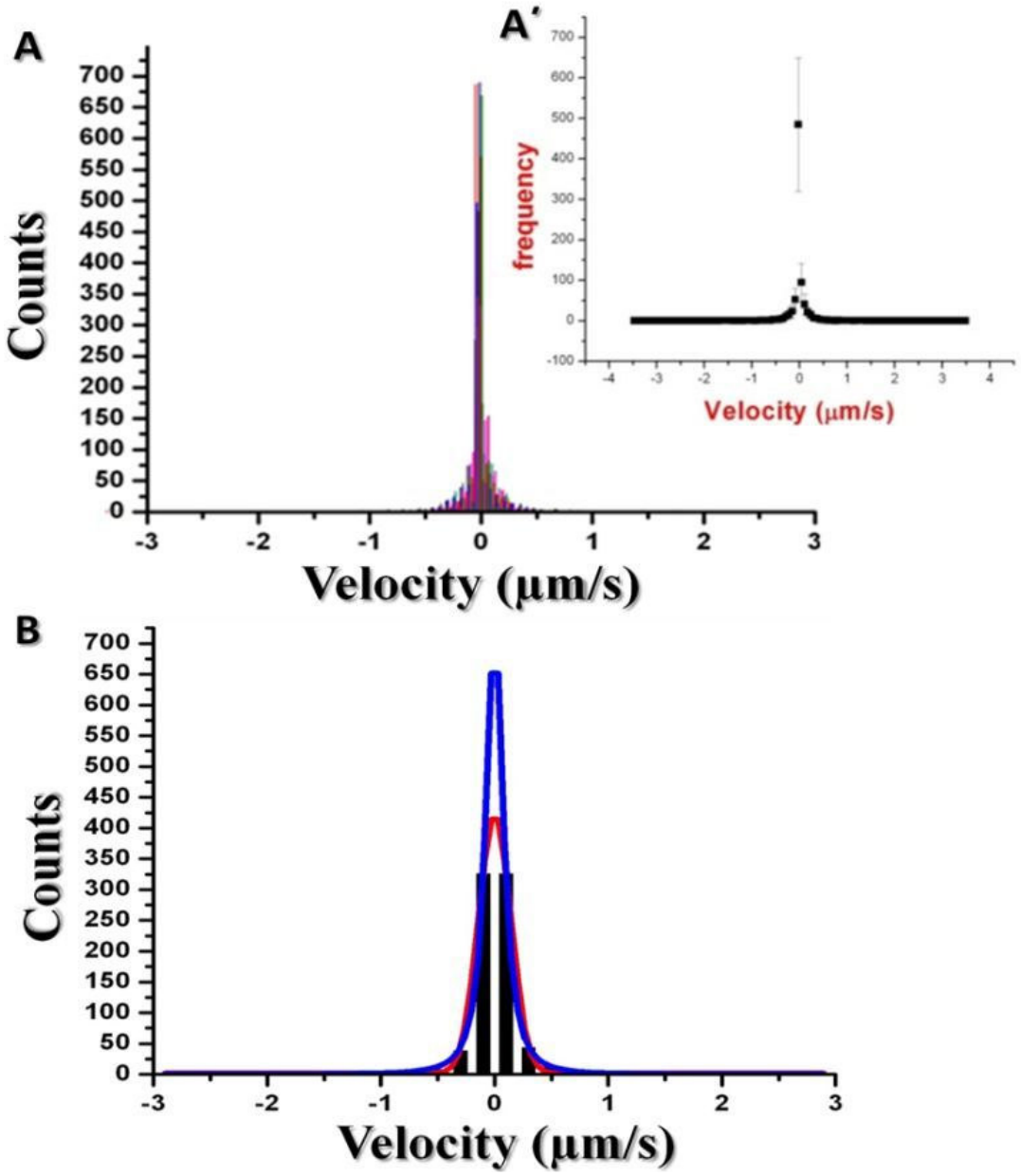

Figure 4. The velocity distribution of GFP-MinE cluster throughout the *E. coli* cell. (A) Shows the histogram plots of GFP-MinE velocity for 10 cell samples. The bin center of the histogram (bin size = 0.2 μm/s) for this data set is shown in the small figure (A'). (B) An example of the fitting curve that corresponds to the histogram in (A). Blue line indicates the Tsallis distribution function (R^2 ~0.99985). Red line indicates the Gaussian distribution function (R^2 ~0.99813).

Gaussian function:

$$F(v) = F_0 + \frac{A}{w\sqrt{\frac{\pi}{2}}} e^{-2\frac{(v-v_c)^2}{w^2}}$$

and, Tsallis function:

$$F_q(v) = A_q[1-(1-q)\frac{\beta m v^2}{2}]^{\frac{1}{1-q}}.$$

We found that the Tsallis distribution function (Upadhyaya et al., 2001; Thurner et al., 2003) appears to be a slightly better fit than the Gaussian function, as shown

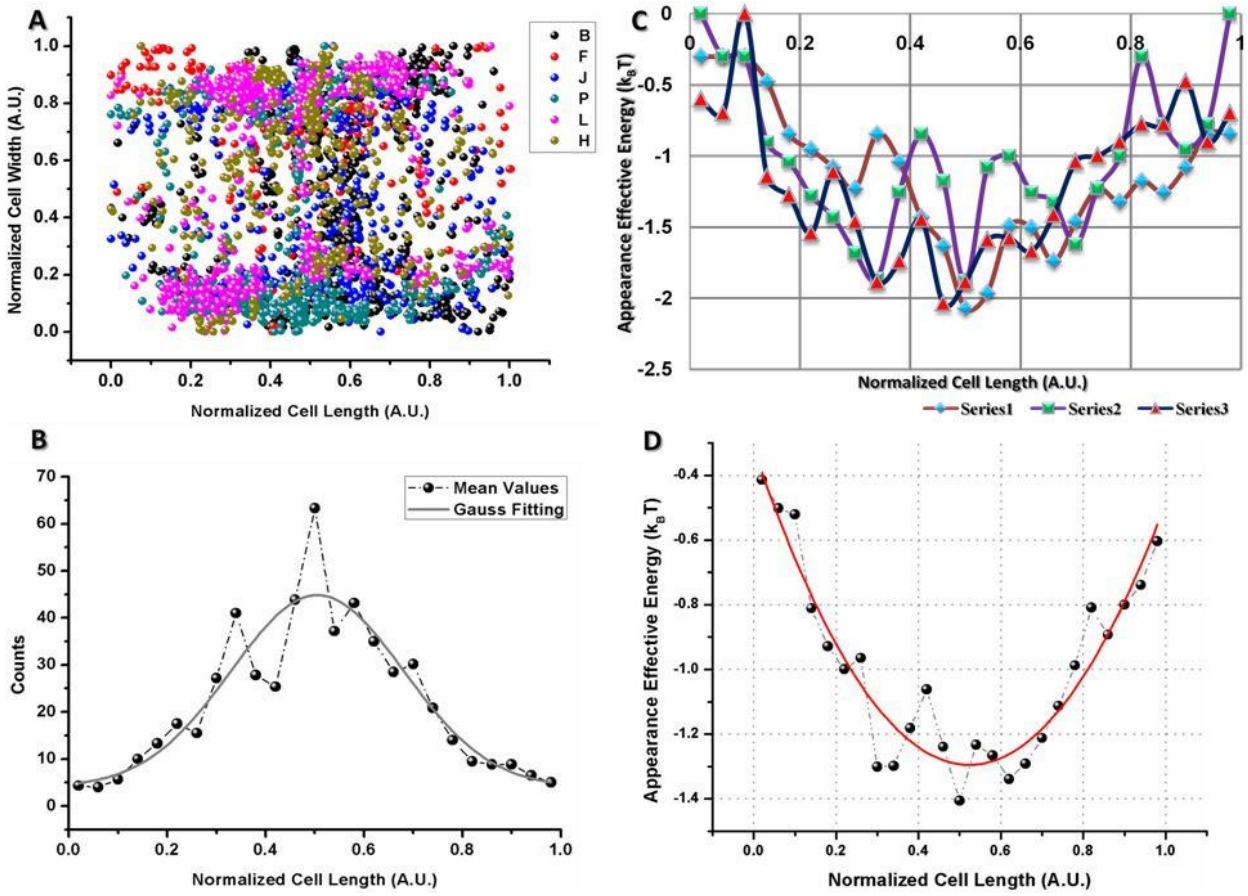

Figure 5. The spatial distribution and energy profile of GFP-MinE cluster. (A) Shows the scattering plots of GFP-MinE (6 cell samples) along normalized cell length and cell width. This figure indicates the MinE cluster positions highly appear at the midcell zone, especially near the cytoplasmic membrane. (B) Shows the spatial distribution of MinE clusters along normalized cell length (for 10 cell samples). Gray line indicates the fitting curve of Gaussian function (R^2 ~ 0.83). (C) Samples of the apparent effective potential profiles for GFP-MinE cluster (3 individual cell samples). (D) Black spots show the average apparent effective potential using the same data set in (B). The red line indicate the spring-like potential fitting function ($y = A+B(x-x_0)^2$), with R^2 ~ 0.97.

in Figure 4B. As seen there, the Gaussian function was not able to cover some data points.

Energy landscape and localization

Here we wanted to analyze the relation between dynamic and geometrical motion, as well as energy landscape. To begin with, we analyzed the motion trajectories of MinE via the scatter plot along the normalized scale. This provides the time, average feature of cluster protein motion and the localization or spatial distribution pattern of cluster protein, as shown in Figure 5A. The cluster protein distributions illustrate characteristic scattering highly near the midcell zone and the edge of cells. This distribution features a ring-like structure forming around the midcell zone. Biologically, this could link to the C-terminal topological specificity domain of MinE principally responsible for allowing the FtsZ ring to form at midcell (King et al., 2000). Our results may also support the evidence of FtsZ protein forming near the midcell zone as a ring structure. Previous reports show that the distribution at gold labeling FtsZ formed a ring-like structure at the division site (Bi and Lutkenhaus, 1991). The FtsZ's self-assemblage into a ring structure on the cytoplasmic surface of the inner membrane may lead to the first step in the division process.

According to the scattering positions of MinE cluster, we then analyzed the cluster protein distribution along normalized cell length, as shown in Figure 5B. These results led to the probability density of finding a cluster molecule at given normalization positions at observable

time frames. We found that the cluster protein distribution was not fitted well by the Gaussian function. However, this fitting function still surprisingly provided us with an approximate central value at around 0.5 (or 50% of cell length). This is consistent with the fact that the possible division site of an *E. coli* cell may occur at midcell. Consequently, we estimated the effective potential associated with MinE motion to increase the understanding of MinE dynamics. The effective potential profiles for individual cluster molecules can be evaluated from $U(x) = -k_B T \log(P(x))$, where $U(x)$ is the effective potential; $P(x)$ is the probability of finding the cluster molecule at position x; and $k_B T$ is the thermal energy (Ritchie et al., 2005; Daumas et al., 2003; Jin et al., 2007; Haken, 1977). It follows then that information about physical, fore-producing mechanisms responsible for diffusive motion of MinE should be contained in STT trajectories, without the need to apply external force. We found that the effective potential relates to the spring-like potential or harmonic potential, as shown in Figures 5C and D. The minimum region indicates the potential depth that occurs near the midcell zone, which corresponds to the finding that the MinE cluster mostly concentrates at midcell. It may be noted that the potential curve is not very smooth and may indicate a metastable state, especially near the midcell zone. This characteristic may reflect the spatial landscape characterizing the environment or cell that interacts with cluster protein motion. Moreover, this metastability may relate to several E-ring structures being formed before they move to the polar zones.

DISCUSSION

The goal of this research was to investigate the dynamics and pattern formations of MinE protein in terms of physical quantities. We focused on two aspects: Dynamic pattern formations and energy landscapes. We then measured the mean square displacement (MSD), velocity distribution, and energy landscape. We performed two major steps to analyze the experimental data (in terms of the image sequence), namely image analysis and STT.

From our results, we found that GFP-MinE clusters occur mostly near the midcell zone, especially near the cytoplasmic membrane (edge of cell), as shown in Figure 1F. They also perform oscillation patterns that take time when moving from the midcell to polar zone as shown in Figure 2A (top). Both of these behaviors could be caused by MinE molecules attaching themselves to the leading edge of MinD-ATP (MinD, ATP polymer grows from the cell poles to cell center near the midcell zone and form the E-ring). MinE in the E-ring activates the MinD-ATP, leading to the conversion of ATP into ADP and the release of phosphate. Consecutive release of MinD-ATP results in depolymerization from the cell center to the cell pole. Also for MinD, the E-ring may perform lateral diffusion in the same direction of the MinD-ATP depolymerization. After this process, MinD-ADP and MinE are released from the cytoplasmic membrane because of its low affinity to the bilayer. MinD-ADP is converted to MinD-ATP in the cytoplasm. And MinD-ATP diffuses to the opposite pole, while MinE moves to the midcell zone by the topological specificity domain (TSD) that is shown to exist as a homodimer in which the long N-terminal α-helices from each monomer form an antiparallel coiled-coil (King et al., 2000). In addition, the fluctuation of MinE clusters that are reflected via trajectories and localizations may come from the polymerization landscapes of MinD protein.

Because the dynamical time scale of MinE cluster movement from the midcell to polar zone and polar zone to midcell are different (Figure 2A), essential protein dynamics and interactions may appear between MinE moves from the midcell to polar zone. This key point may relate to FtsZ diffusion (Niu and Yu, 2008). To understand these results, we measured MSD and velocity distribution.

In order to consider the MSD, we found that the GFP-MinE cluster motion performed the fractional diffusion-advection second moment with $\alpha = 0.44 \pm 0.25$. These results indicated that GFP-MinE clusters perform subdiffusion at the short time and directed motion at the long time. This finding could well be related to a previous report on the diffusion of MinD proteins (Unai et al., 2009). There, they found that GFP-MinD clusters perform subdiffusion with dynamic exponents approximately 0.34 ± 0.18. It was understood that MinD and MinE were involved in a biochemical kinetic interaction within an *E. coli* wherein MinD generated polymerization on the cytoplasmic membrane (Hu and Lutkenhaus, 2001; Suefuji et al., 2002) and grew from the cell poles to cell center (Taghbalout et al., 2006; Rothfield et al., 2005), while MinE enacted depolymerization by firstly attaching to the leading edge of MinD-ATP near the midcell and then moving to the polar zone (Figure 1E, F, A and A).

These results could be expanded MinE behaviors in terms of directed motion. Subdiffusion of MinE may also be related to MinD polymerization landscapes and interactions, especially on the cytoplasmic membrane. Moreover, a recent report on FtsZ protein indicates that it performed subdiffusion where $\alpha = 0.74 \pm 0.05$ (Niu and Yu, 2008). This action facilitated the subdiffusive feature of MinE. Because MinE is principally responsible for allowing the FtsZ to form at midcell (King et al., 2000), this situation possibly appears in the area outside the midcell zone that is related to the area outside of the Z-ring. To validate our point, we use the histogram of

effective diffusion coefficients. It appears that the most effective diffusion coefficient values are small, and the histogram of effective diffusion coefficients can not be fitted with the Gaussian function, as shown in Figure 3D. This result may indicate the effect of environments and the protein mechanism, which may imply the memory effect or long range correlation of protein cluster movement that leads to anomalous subdiffusion. The average of effective diffusion coefficients is approximately $0.20\pm0.16\ \mu m^2/s^{0.44\pm0.25}$.

According to the Tsallis distribution function, q-values indicate the correlation of particle motion. In our experiments, q-values are approximately 1.55±0.037, showing a connection of q>1 and correlated motion (correlated diffusion in terms of fractional Brownian motion). Recalling the relation between q-values and dynamic exponents in anomalous diffusion, $\alpha = 2/(3-q)$ (Upadhyaya et al., 2001; Thurner et al., 2003; Fuentes and Cáceres, 2008); we then have the dynamic exponent α = 1.41±0.037. It is seen that the dynamic exponent is not equal to the one that results from MSD estimation. In fact, the estimated exponent here is about double of that via MSD estimation. This result may reflect the symmetry of the dynamic exponent, which takes into account the characteristics of a moving path (Figures 1E and 2A) that performs the symmetry pattern along the cell length (midcell zone represents the central point). Since the GFP-MinE cluster is in such close contact with the cytoplamic membrane (according to the polymerization mechanism of MinD proteins), it leads to anomalous subdiffusion, which indicates the correlation of motion via q-values.

By inspection, we fitted the MinE potential profile using the estimated function $y = A + B(x - x_0)^2$, as shown in Figure 5D. The average potential depth for curve fitting was found to be $U_0 \approx 0.92\, k_B T$, which is quite a reasonable order of magnitude as far as thermal fluctuation is concerned. This parameter seems to the energy that required generating the pattern formation of MinE cluster dynamics. Next we used Kramers's escape problem (Kramers, 1940) concerning a point particle in phase space diffusing in the potential. Given a medium or space where a particle is caught in a potential hole, the particle can only escape over a potential barrier. Hence this model was used mainly to study the dependence of the escape rate on temperature and viscosity. In this regard, we assumed the probability of random moving particles over the potential U at each position as: $P(U) = \frac{1}{U_0} e^{-U/U_0}$. Considering *the rate of escape,* (Kramers, 1940) r_e where $r_e \to 0$ and $\tau_e \to \infty$), we adopted the approximation: $r_e \approx e^{\frac{U}{k_B T}}$, which is valid at the low $k_B T$ limit. The *mean waiting time to escape* (τ) may thus be written as: $\tau \approx \tau_0 e^{\frac{U}{k_B T}} \approx 1/r_e$. Applying the estimated waiting time distribution τ between steps (Scher et al., 1991; Saxton, 1996) using: $\psi(\tau) = P(U)\frac{dU}{d\tau}$. We arrive at $\psi(\tau) \approx \tau^{-(1+\frac{k_B T}{U_0})}$. Hence, from the waiting time PDF (Metzler and Klafter, 2000; Wong et al., 2004), we get $\alpha = \frac{k_B T}{U_0}$, where α corresponds with the dynamic exponent for the subdiffusive case $0 < \alpha < 1$. According to the symmetrical dynamics of MinE cluster, it was supported by the dynamic exponent of velocity distribution. We also found that the dynamic exponent of the average potential depth is approximately 0.5. This parameter indicated the subdiffusive motion of MinE cluster at the half cell length, which correspond to the subdiffusive motion of MSD at the same region.

Key questions that remain to be addressed are the effects of different types of culture conditions, various stresses, and time and space dependent noises on MinE dynamics and the stabilization of patterns. On the STT side, the crucial question still concerns to what extent this technique will precisely be used to investigate protein cluster dynamics. A lot more work needs to be done to test and reach the limit of this method. To advance the theory and modeling, it is also necessary to make use of these quantitative results and experimentally testable predictions, where possible.

In conclusion, a spot tracking technique (STT) was used here to track the maximum distribution of a particle ensemble, making it possible to observe, both qualitatively and quantitatively, MinE dynamics. The main results were used to quantitatively analyze dynamic pattern formation and energy landscape. An interesting characteristic of time evolution dynamics is the flight event that occurs between polar zones and midcell, a behavior that is still not well understood. In terms of MinE localization, by analyzing the cluster positions using the STT technique, patterns of localization and distribution along the cell length have been well confirmed, while other quantitative information related to MinE cluster positions have been revealed. In addition, the effective potential was found to relate to the spring-like potential or harmonic potential. The minimum region indicated the potential depth that occurs near the midcell

zone, which corresponds to the finding that the MinE cluster mostly concentrates at midcell.

It is reasonable to say that with the STT technique, the measurements performed are more accurate than those done by, say eye-observed measurement in a 2D-image sequence. However, the accuracy of this STT may be subject to environmental factors. We believe that STTs will be widely applied to Min protein systems in the very near future. With improvements in STTs, through data acquisition and data analysis, the STT could become a well-accepted technique. Furthermore, the combined use of STT with the well-known technique of fluorescent labeling or dyeing could be a promising alternative to other types of labeling, including the nanoparticle labeling approach. It is also reasonable to say that this quantitative information could contribute to improvements in the dynamic model of protein oscillation. It is important to emphasize that obtaining the quantitative data of protein dynamics is one of the distinct rewards owed to this applied STT. As improvements are made to the STT technique, especially applications in 3D, the information to be gained may reflect as yet unproven mechanisms, such as an obstruction of MinE by other mobile or immobile molecules or by other Min proteins, binding and obstruction by cellular components.

ACKNOWLEDGEMENTS

The authors thank David Blyler for editing the manuscript and our biophysics group members for reading the manuscript and providing helpful comments. Technical assistance by Somruthai Kidsanguan at the Institute of Molecular Biosciences is also acknowledged. This research project is supported by Faculty of Science, Mahidol University, The Center of Excellence for Innovation in Chemistry (PERCH-CIC), Thailand Research Fund (TRF), and Commission on Higher Education (CHE).

REFERENCES

Bi EF, Lutkenhaus J (1991). FtsZ ring structure associated with division in *Escherichia coli*. Nature, 354: 161-164.

Daumas F, Destainville N, Millot C, Lopez A, Dean D, Salome L (2003). Confined diffusion without fences of a G-protein-coupled receptor as revealed by single particle tracking. Biophys. J., 84: 356–366.

de Boer PAJ, Crossley RE, Rothfield L I (1989). A division inhibitor and a topological specificity factor coded for by the minicell locus determine proper placement of the division septum in *E. coli*. Cell, 56: 641–649.

Fu X, Shih YL, Zhang Y, Rothfield L I (2001). The MinE ring required for proper placement of the division site is a mobile structure that changes its cellular location during the *Escherichia coli* division cycle. Proc. Natl. Acad. Sci., USA, 98: 980–985.

Fuentes MA, Cáceres MO (2008). Computing the non-linear anomalous diffusion equation from first principles. Phys. Lett. A., 372: 1236-1239.

Golding I, Cox EC (2006). Physical Nature of Bacterial Cytoplasm. Phys. Rev. Lett., 96: 098102-098105.

Haken H (1977). Synergetics: An Introduction. Nonequilibrium Phase-Transitions and Self-Organization in Physics, Chemistry and Biology (Springer).

Hale CA, Meinhardt H, de Boer PAJ (2001). Dynamics localization cycle of the cell division regulator MinE in *Escherichia coli*. EMBO J., 20: 1563-1572.

Hu Z, Lutkenhaus J (1999). Topological regulation of cell division in *Escherichia coli* involves rapid pole to pole oscillation of the division inhibitor MinC under the control of MinD and MinE. Mol. Microbiol., 34: 82-90.

Hu Z, Lutkenhaus J (2001). Topological regulation of cell division in *E. coli*: spatiotemporal oscillation of MinD requires stimulation of its ATPase by MinE and phospholipids. Mol. Cell, 7: 1337-1343.

Jin S, Haggie PM, Verkman AS (2007). Single-Particle Tracking of Membrane Protein Diffusion in a Potential: Simulation, Detection, and Application to Confined Diffusion of CFTR Cl^- Channels. Biophys. J., 93: 1079-1088.

Janthon U, Unai S, Kanthang P, Ngamsaad W, Modchang C, Triampo W , Krittanai C, Wtriampo D and Lenbury Y (2008). Single-Particle Tracking Method for Quantitative Tracking and Biophysical Studies of the MinE Protein. JKPS, 52: 639-648.

Justice SS, Garcia-Lara J, Rothfield LI (2000). Cell division inhibitors SulA and MinC/MinD block septum formation at different steps in the assembly of the *Escherichia coli* division machinery. Mol. Microbiol., 37: 410-423.

King GF, Shih Y-L, Maciejewski MW, Bains NPS, Pan B, Rowland SL, Mullen GP, Rothfield LI (2000). Structural basis for the topological specificity function of MinE. Nat. Struct. Biol., 7: 1013-1017.

Kramers HA (1940). Brownian motion in a field of force and the diffusion model of chemical reactions. Physica, 7: 284-286.

Lutkenhaus J, Addinall SG (1997). Bacterial cell division and the Z ring. Annu. Rev. Biochem., 66: 93-116.

Metzler R, Klafter J (2000). The random walk's guide to anomalous diffusion: a fractional dynamics approach. Phys. Rep., 339: 1-77.

Niu L, Yu J (2008). Investigating Intracellular Dynamics of FtsZ Cytoskeleton with Photoactivation Single-Molecule Tracking. Biophys. J., 95: 2009-2016.

Qian H, Scheetz M, Elson E L (1991). Single particle tracking. Biophys. J., 60: 910-921.

Raskin DM, de Boer PAJ (1999). MinDE-dependent pole-to-pole oscillation of division inhibitor MinC in *Escherichia coli*. J. Bacteriol., 181: 6419-24.

Raskin DM, de Boer PAJ (1999). Rapid pole-to-pole oscillation of a protein required for directing division to the middle of *Escherichia coli*. Proc. Natl. Acad. Sci. USA, 96: 4971-4976.

Ritchie K, Shan X-Y, Kondo J, Iwasawa K, Fujiwara T, Kusumi A (2005). Detection of Non-Brownian Diffusion in the Cell Membrane in Single Molecule Tracking. Biophys. J., 88: 2266–2277.

Rothfield L, Justice S, Garcia-Lara J (1999). Bacterial cell division. Annu. Rev. Genet., 33: 423-448.

Rothfield LI, Shih Y-L, King G (2001). Polar explorers: membrane proteins that determine division site placement. Cell, 106: 13-16.

Rothfield L, Taghbalout A, Shih Y –L (2005). Spatial control of bacterial division-site placement. Nat. Rev. Microbiol., 31: 959-968.

Rowland SL, Fu X, Sayed MA, Zhang Y, Cook WR, Rothfield L (2000). Membrane redistribution of the *Escherichia coli* MinD protein induced by MinE. J. Bacteriol., 182: 613-619.

Sage D, Neumann FR, Hediger F, Gasser SM, Unser M (2005). Automatic tracking of individual fluorescence particles: Application to the study of chromosome dynamics. IEEE Trans. Image Process., 14: 1372-1383.

Saxton MJ (1996). Anomalous diffusion due to binding: A Monte Carlo study. Biophys. J., 70: 1250–1262.

Saxton MJ, Jacobson K (1997). Single-particle tracking: Applications to membrane dynamics. Ann. Rev. Biophys. Biomol. Struct., 26: 373-399.

Scher H, Shlesinger MF, Bendler JT (1991). Time-scale invariance in transport and relaxation. Phys. Today, 44: 26-34.
Shih Y -L, Le T, Rothfield L (2003). Division site selection in *Escherichia coli* involves dynamic redistribution of Min proteins within coiled structures that extend between the two cell poles. Proc. Natl. Acad. Sci. USA,, 100: 7865-7870.
Shih Y-L, Rothfield LI (2006). The Bacterial Cytoskeleton. MMBR, 70: 729-754.
Suefuji K, Valluzzi R, RayChaudhuri D (2002). Dynamic assembly of MinD into filament bundles modulated by ATP, phospholipids, and MinE. Proc. Natl. Acad. Sci. (USA), 99: 16776-16781.
Suzuki K, Ritchie K, Kajikawa E, Fujiwara T, Kusumi A (2005). Rapid hop diffusion of a G-protein-coupled receptor in the plasma membrane as revealed by single-molecule techniques. Biophys. J., 88: 3659-3680.
Taghbalout A, Ma L, Rothfield LI (2006). Role of MinD-Membrane Association in Min Protein Interactions. J. Bacteriol., 188: 2993-3001.
Thurner S, Wickc N, Hanele R, Sedivyc R, Huber L (2003). Anomalous diffusion on dynamical networks: A model for interacting epithelial cell migration. Physica A., 320: 475-484.
Tolic´-Nørrelykke IM, Munteanu E-L, Thon G (2004). Anomalous Diffusion in LivingYeast Cells. Phys. Rev. Lett., 93: 078102-1.
Unai S, Kanthang P, Junthon U, Ngamsaad W, Triampo W, Modchang C, Krittanai C (2009). Quantitative analysis of time-series fluorescence microscopy using a spot tracking method: Application to Min protein dynamics. Biologia, 64: 27-42.
Upadhyaya A, Rieub J-P, Glaziera JA, Sawada Y (2001). Anomalous diffusion and non-Gaussian velocity distribution of Hydra cells in cellular aggregates. Physica A., 293: 549-558.
Yu XC, Margolin W (1999). FtsZ ring clusters in min and partition mutants: Role of both the Min system and the nucleoid in regulating FtsZ ring localization. Mol. Microbiol., 32: 315-326.
Woldringh CL, Mulder E, Huls PG, Vischer N (1991). Toporegulation of bacterial division according to the nucleoid occlusion model. Res. Microbiol., 142: 309-320.
Wong IY, Gardel M L, Reichman DR, Weeks ER, Valentine MT, Bausch AR, Weitz DA (2004). Anomalous Diffusion Probes Microstructure Dynamics of Entangled F-Actin Networks. Phys. Rev. Lett., 92: 178101-1.